



Simultaneous and Spontaneous Oxidation and Reduction in Microdroplets by the Water Radical Cation/Anion Pair

Lingqi Qiu and R. Graham Cooks*

Abstract: Microdroplets show unique chemistry, especially in their intrinsic redox properties, and to this we here add a case of simultaneous and spontaneous oxidation and reduction. We report the concurrent conversions of several phosphonates to phosphonic acids by reduction ($R-P \rightarrow H-P$) and to pentavalent phosphoric acids by oxidation. The experimental results suggest that the active reagent is the water radical cation/anion pair. The water radical cation is observed directly as the ionized water dimer while the water radical anion is only seen indirectly through the spontaneous reduction of carbon dioxide to formate. The coexistence of oxidative and reductive species in turn supports the proposal of a double-layer structure at the microdroplet surface, where the water radical cation and radical anion are separated and accumulated.

Microdroplet chemistry is a relatively new field that has engendered much recent interest and the topic has been reviewed.^[1,2] Chemical reactions in micron-sized droplets under ambient conditions are often orders of magnitude faster than the equivalent bulk reactions.^[3-9] The catalyst-like role of microdroplets makes them excellent tools for rapid chemical derivatization^[10,11] and small-scale synthesis.^[3,12-17] The observed reaction acceleration is explained by the peculiar environment at the droplet air/solution interface, where reactants are only partially solvated^[1,2,18,19] and which is characterized by a high electric field.^[20-23] Both these features strongly influence the rates of reactions intrinsic to the chosen reagents, but they may also activate solvent molecules at the interface and this can result in microdroplet-specific reactions that are distinct from ordinary bulk reactions. Two fundamental processes have been considered to be involved in aqueous microdroplet redox chemistry: (i) Disproportionation of hydroxide due to the electric field to give hydroxyl radical and electron, resulting in spontaneous oxidation^[24-27] and reduction;^[28,29]

and (ii) dissociation of the radical cation/anion pair ($H_2O^+ \bullet / H_2O^{\bullet -}$), recently argued to exist in pure bulk water,^[30] to provide the free radical cation and radical anion.^[26,27,31] Notably, *simultaneous* oxidation and reduction in microdroplets has not yet been reported; such an observation would support the second source of reactive species in water microdroplets.

Phosphonates comprise a minor fraction of total organic phosphorus,^[32] but are highly significant in biochemistry.^[33] On the one hand, through enzymatic carbon-phosphorus (C-P) bond cleavage, phosphonates can serve as the phosphorus source for the creation of biologically important molecules, e.g. adenosine triphosphate.^[34] On the other hand, some organophosphorus compounds, such as the chemical agent Sarin, are highly toxic. Consequently, research on phosphonates, particularly on their spontaneous interconversions, is important for an understanding of their transformations, including their degradation in biological systems.

In this study, we present evidence for the simultaneous and spontaneous oxidation and reduction of phosphonates to the corresponding phosphoric and phosphonic acids. We show evidence that the water radical cation/anion pair acts as both oxidant and reductant when pure water is sprayed. The result suggests that the oxidative and reductive species can coexist in a microdroplet and trigger opposite but simultaneous reactions. The recent suggestion of a double-layer structure at the droplet surface^[19,35-38] accounts for the co-occurrence of these two reactions with separation of the water radical cation/anion pairs into free ions by the strong electric field which also acts to accumulate them in oppositely-charged surface layers.

A solution of dimethyl methylphosphonate (**1a**) in water was sprayed and analyzed using nano-electrospray ionization mass spectrometry (nESI-MS); the spectra obtained in the positive and negative modes are displayed in Figure 1. The water radical cation adduct (**2a**) was observed at m/z 142. This observation is consistent with a high-throughput DESI-MS analysis of a library of 21 000 non-proprietary chemicals, in which water radical cation adducts ($[M+H_2O]^+\bullet$) of significant intensity were found in 65 % of all the X=Y double bond-containing compounds.^[27] Replacing water by heavy water (D_2O) gave the corresponding deuterated ions (Figure 1c) while $[M+18]^+\bullet$ was still seen due to rapid H-D exchange. Tandem mass spectrometry (see Figure S1 in Supporting Information) showed that the water adduct, $RP(OR)_2(OH)_2^+\bullet$, is covalently bound. Strikingly, in the negative mode, a product at m/z 95 was found and shown by MS/MS analysis to fragment by neutral loss of MeOH which

[*] L. Qiu, Dr. R. G. Cooks

Department of Chemistry, Purdue University
 560 Oval. Dr., West Lafayette, IN 47907 (USA)
 E-mail: cooks@purdue.edu

© 2022 The Authors. Angewandte Chemie International Edition published by Wiley-VCH GmbH. This is an open access article under the terms of the Creative Commons Attribution Non-Commercial NoDerivs License, which permits use and distribution in any medium, provided the original work is properly cited, the use is non-commercial and no modifications or adaptations are made.

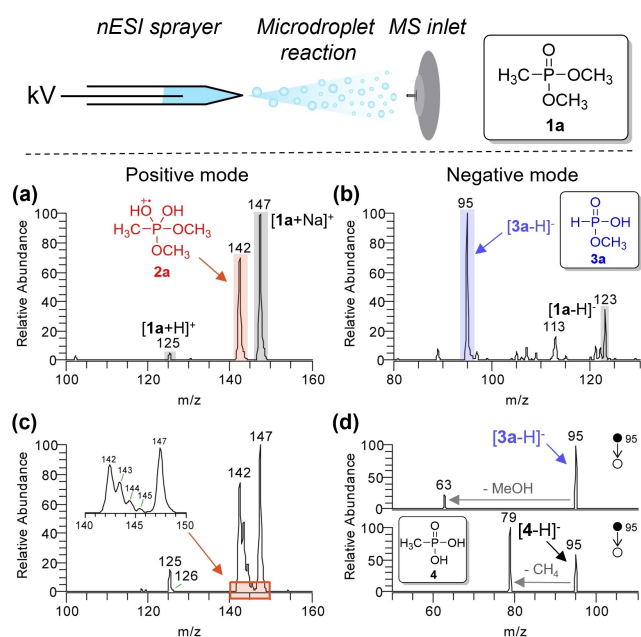


Figure 1. Oxidation and reduction of DMMP (**1a**). Solutions of DMMP in water were converted to microdroplets by nESI and the ionized products were directly detected by MS. Mass spectra in a) positive mode and b) negative mode, 10 mM phosphonate **1a** at spray distance of 5 mm, showing the oxidation and reduction products at m/z 142 and 95, of different polarities. c) Mass spectrum of 10 mM phosphonate **1a** in heavy water in the positive mode. d) Distinctive MS/MS spectra of the reduction product (assigned as **3a**) and its isomer **4**, showing characteristic neutral losses of MeOH and CH_4 , respectively.

characterizes it as reduced product **3a** (Figure 1d, top panel).^[39] Although complete hydrolysis of phosphonate **1a** can produce methylphosphonic acid **4**,^[40] the distinctive MS/MS spectrum (Figure 1d) of the reaction product (**3a**) compared to authentic methylphosphonic acid (**4**) confirms that the generated product at m/z 95 is not the methylphosphonic acid. To rule out the possibility of contributions from electrochemical reactions near the electrode,^[41–43] inductive nESI (without physical contact between solution and electrode), was performed and peaks at m/z 142 (positive) and 123 (negative mode) were still observed (see Supporting Information, Figure S2).

We also investigated the effect of changes in the concentration of **1a** in water and of the distance between the sprayer and MS inlet upon the reduction reaction. Increased concentration gave the predicted increase in conversion to yield the reduced product (see Supporting Information, Figure S3a). The extended spray distance also produced higher conversion to product, as a result of the longer reaction time and the smaller microdroplets generated from the spray (see Figure S3b).^[44] This result, as well as the fact that negligible conversion was observed in the corresponding bulk reaction (2 mL, 72 hours) (see Figure S4), indicates that the reduction occurs in microdroplets.

To explore further the mechanism underlying the observed oxidation, viz. the generation of the adduct of phosphonate and water radical cation, and the reduction, viz. the yield of phosphonic acid, several comparisons were

made. A key question concerns the actual oxidant, with the candidates being (i) water radical cation and (ii) hydroxyl radical, as noted in the introduction. To answer the question, reactions of **1a** were compared in the presence and absence of 15% H_2O_2 and the outcome is displayed in Figure 2a. In the presence of H_2O_2 , the protonated phosphonate signal ($[\mathbf{1a}+\text{H}]^+$) increased relative to the water radical cation adduct, likely due to the higher Brønsted acidity of H_2O_2 than water. A similar pattern was found (Figure 2b) when pure water and 15% H_2O_2 aqueous solution were compared without adding the phosphonate reagent **1a**. Protonation is favored by introducing H_2O_2 into the reaction system, suggesting that the strong signals for $[\mathbf{1a}+\text{H}_2\text{O}]^{+\bullet}$ observed for the **1a** aqueous solution, as well as that for $(\text{H}_2\text{O}_2)^{+\bullet}$ in pure water, are not associated with peroxide. Further evidence for this is the detection of the ion at m/z 34, which is assigned as $\text{H}_2\text{O}_2^{+\bullet}$ but not seen in pure water. We conclude that the radical cation is the oxidant.

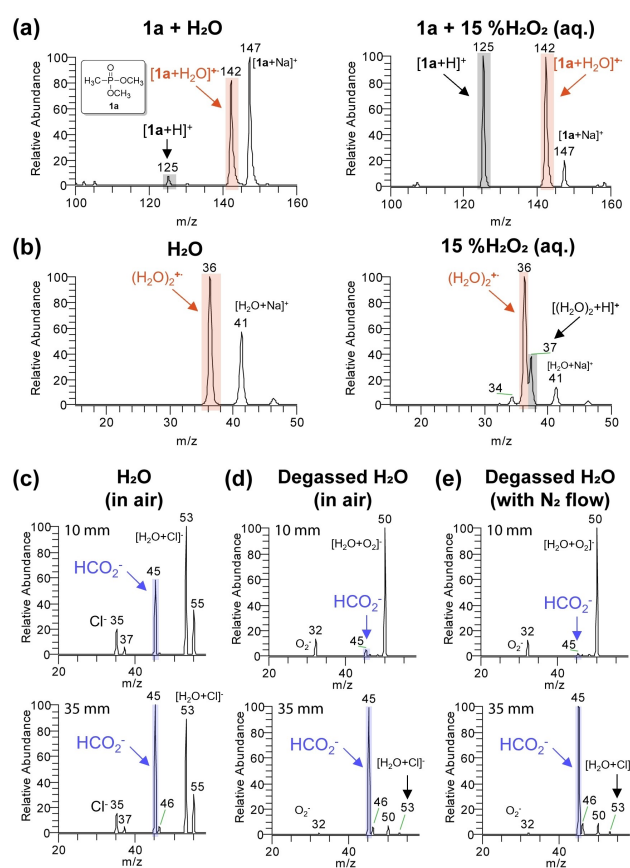


Figure 2. Mechanistic investigation of oxidizing and reducing species in water a) Comparison of positive mode spectra of **1a** (10 mM) with and without 15% H_2O_2 in aqueous solution; protonated **1a** at m/z 125 and oxidized **1a** at m/z 142 are highlighted. b) Comparison of positive ion spectra of pure water and 15% H_2O_2 aqueous solution. Mass spectra in negative mode of c) pure water, d) degassed pure water (N_2 used to degas the water) sprayed in air and e) degassed water with a N_2 gas atmosphere, showing the signal due to formic acid, superoxide and adventitious chloride ions. More formate was seen in (c), (d), and (e) when the spray distance was increased from 10 mm to 35 mm.

In the negative mode, an intriguing signal at m/z 45 was observed (Figure 2c), presumably due to formic acid generated by reduction of carbon dioxide from either dissolved CO_2 in water or in air. To explore the CO_2 source, pure water degassed by N_2 , was sprayed and a weak formate signal was observed, indicating a contribution from dissolved CO_2 (Figure 2c). Later, as N_2 gas was introduced near the sprayer, the expected decrease in HCO_2^- was found, suggesting that ambient CO_2 is also involved in formic acid generation. The distance effect shown in Figure 2c–e, viz. longer spray distances (e.g. 35 mm) yield much higher formate ion intensities, confirms the participation of CO_2 in air. To validate the fact that formic acid is produced from CO_2 , we provide a CO_2 -rich environment for the water microdroplets, and a clear response of the formate signal to CO_2 “on” and “off” was found (see Supporting Information, Figure S5). This reaction suggests the possibility of application of microdroplets in CO_2 fixation;^[37,45] to the best of our knowledge there is no precedent for this in the literature. Inductive nESI analysis was performed and both the water radical cation and formic acid were identified (see Supporting Information, Figure S6). Processes explaining the observed ions are illustrated. Our evidence suggests that the primary reactive species in the positive and negative modes are the water radical cation and the water radical anion (the hydrated electron), respectively, and that water is the source of both ions. We see no evidence for hydroxy radical as a reagent although we do not exclude it.

Although the intrinsic redox characteristics of water microdroplets are demonstrated by the above results, the products of oxidation and reduction were identified by measurements made using different ion polarities. A stronger case could be made by using a single polarity measurement to observe products of both reduction and oxidation. When a solution of **1a** in acetonitrile (not intentionally dried) was sprayed, three different types of products were seen (Figure 3) in the negative mode: the phosphonic acid **3a** formed by reduction, the alkyl phosphonic acid **5a** by hydrolysis, and the phosphoric acid **6a** by oxidation. The failure to observe the acidic products in the positive mode is simply explained by their low ionization efficiency, given that no external proton source was provided in this experiment. A lower ratio of $[\mathbf{1a} + \text{H}_2\text{O}]^+ / [\mathbf{1a} + \text{H}]^+$ was found in acetonitrile compared to water. Moreover, no deprotonated reactant (**4a**) was observed. The differences between water and acetonitrile microdroplets (which include traces of water) cause different local concentrations of phosphonate and water at the droplet surface where the water radical cation is thought to be generated.^[26,46,47] In solutions with only traces of water, the generated water radical cation has a good chance to first encounter and oxidize phosphonate. By contrast, in water microdroplets, the water radical cation would most likely first encounter neighboring water molecules, producing the hydronium cation and hydroxyl radical. The lower oxidizing power of hydroxyl radical compared to the water radical cation^[48] results in the absence of oxidation products in water microdroplets.

Other phosphonates, including diethyl methylphosphonate (**1b**), diisopropyl methylphosphonate (**1c**),

diethyl difluoromethyl phosphonate (**1d**), diethyl phenylphosphonate (**1e**) and diphenyl phenylphosphonate (**1f**) were explored in acetonitrile microdroplets, and the corresponding products from reduction, hydrolysis and oxidation were seen and are marked in figure 3. In all alkyl phosphonate cases, the oxidation products were observed except for **1d**, where the high electronegativity of the difluoromethyl group makes oxygen insertion difficult. The reduction reaction occurred in **1a** to **1e**, suggesting the need for alkyl groups on the phosphonates. By contrast, the aryl group-rich substrate **1f** showed the highest $[\text{M} + \text{H}_2\text{O}]^+ / [\text{M} + \text{H}]^+$ ratio but the absence of a reduction product. These facts suggest that the substituents on the reactants greatly affect the outcome of the redox reactions. The proposed oxidation mechanism, which is analogous to the spontaneous oxidation of the carbon-heteroatom double bond in microdroplets,^[26,27] involves the production of the water radical cation adduct, followed either by direct homolysis of the P–C bond or by 1,2-migration and then C–O cleavage (see Supporting Information, Figure S7). The reduction mechanism is still under investigation.

Simultaneous reduction and oxidation was observed at the same polarity, suggesting that the oxidizing and reducing species must coexist in the analyzed microdroplets. This in turn suggests a double-layer model for the structure of the charged microdroplets. As illustrated in figure 4, the conversion from water molecules to the water radical cation/anion pair and then to the highly reactive free cations and anions will be promoted by the strong electric field known to exist near the droplet surface.^[19,35–37] Due to their opposite polarities, these free ions will be accumulated in different layers and produce the double-layer structure. The outer layer is enriched in the water radical cation, which gives it strong oxidative abilities to convert phosphonate into phosphoric acid derivatives. The inner layer accumulates water radical anion, thus presenting highly reductive properties that allow the generation of phosphonic acid. If the polarity of the droplet is changed a similar structure will result but with outer reductive layer and inner oxidative layer. The redox layer enables the simultaneous oxidation and reduction events even at the same polarity.

In summary, we report the simultaneous and spontaneous oxidation and reduction of phosphonates in microdroplets. The intrinsic redox properties of water microdroplets is demonstrated by the generation of water dimer radical cation as well as formic acid (from the reduction of carbon dioxide in air). Importantly, the reduction and oxidation of phosphonate to phosphonic acid and phosphoric acid was observed in acetonitrile microdroplets at the same polarity, indicating that the oxidative and reductive species must coexist in the same microdroplets. This result supports a double-layer model,^[19,35–38] where the strong electric field aids the dissociation of the water radical cation/anion pair to free ions as well as enrichment of oppositely charged ions in separate layers. As a result of oxidizing and reducing layers being established, oxidation and reduction occur simultaneously. The spontaneous conversion of phosphonate, involving oxidation and reduction

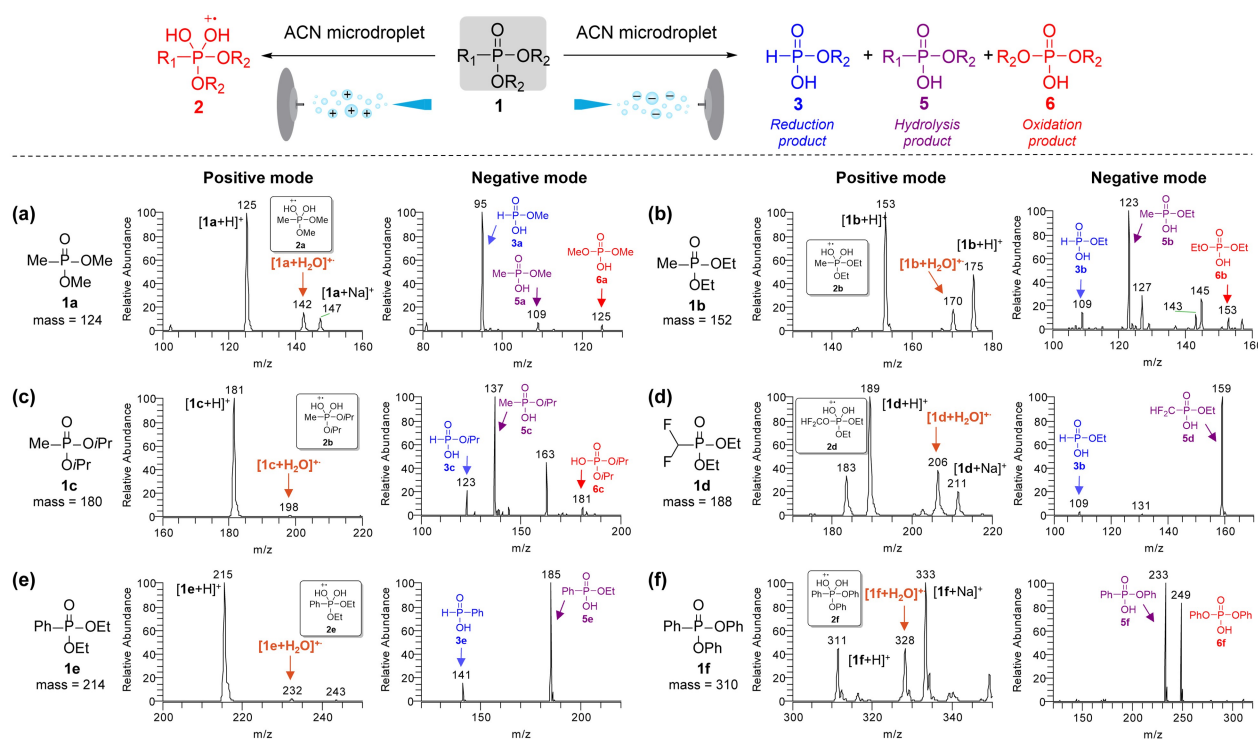


Figure 3. Spontaneous oxidation and reduction of phosphonates **1** (10 mM) in acetonitrile solution (containing traces of water). In the positive mode, the water radical cation adduct **2** was observed. In the negative mode, three types of products were observed simultaneously, **3** from reduction, **5** from hydrolysis and **6** from oxidation, marked in blue, purple and red, respectively. The mass spectra of **1a–1f** are shown in (a) to (f).

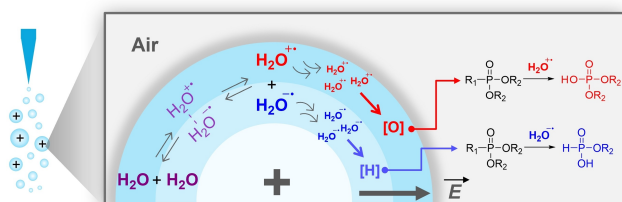


Figure 4. Double-layer model for simultaneous oxidation and reduction in microdroplets. The strong electric field promotes the natural dissociation of water into radical cation/anion pairs^[30] and separates the free radical ions into different layers, enabling oxidation at the outer layer via water radical cations and reduction in the inner layer via water radical anions.

as well as hydrolysis, could provide new insights into its biological transformations.

Acknowledgements

The authors acknowledge financial support from the Multi-University Research Initiative (MURI) of the Air Force Office of Scientific Research (FA9550-21-1-0170) via Stanford University (sub-award 62741613-204669) and also support from the National Science Foundation (grant CHE-1905087).

Conflict of Interest

The authors declare no conflict of interest.

Data Availability Statement

The data that support the findings of this study are available from the corresponding author upon reasonable request.

Keywords: Interfacial Chemistry · Mass Spectrometry · Microdroplets · Phosphonates · Water Radical

- [1] X. Yan, R. M. Bain, R. G. Cooks, *Angew. Chem. Int. Ed.* **2016**, *55*, 12960–12972; *Angew. Chem.* **2016**, *128*, 13152–13166.
- [2] Z. Wei, Y. Li, R. G. Cooks, X. Yan, *Annu. Rev. Phys. Chem.* **2020**, *71*, 31–51.
- [3] T. Müller, A. Badu-Tawiah, R. G. Cooks, *Angew. Chem. Int. Ed.* **2012**, *51*, 11832–11835; *Angew. Chem.* **2012**, *124*, 12002–12005.
- [4] E. A. Crawford, C. Esen, D. A. Volmer, *Anal. Chem.* **2016**, *88*, 8396–8403.
- [5] K. J. Vannoy, I. Lee, K. Sode, J. E. Dick, *Proc. Natl. Acad. Sci. USA* **2021**, *118*, e2025726118.
- [6] N. Sahota, D. I. AbuSalim, M. L. Wang, C. J. Brown, Z. Zhang, T. J. El-Baba, S. P. Cook, D. E. Clemmer, *Chem. Sci.* **2019**, *10*, 4822–4827.
- [7] W. Zhang, B. Zheng, X. Jin, H. Cheng, J. Liu, *ACS Sustainable Chem. Eng.* **2019**, *7*, 14389–14393.

- [8] P. Basuri, J. S. Kumar, S. Das, T. Pradeep, *ACS Sustainable Chem. Eng.* **2022**, *10*, 8577.
- [9] J. Wei, J. Sun, Y. Yin, N. Zeng, J. Ouyang, N. Na, *Int. J. Mass Spectrom.* **2022**, *471*, 116754.
- [10] H. Chen, I. Cotte-Rodríguez, R. G. Cooks, *Chem. Commun.* **2006**, 597.
- [11] Z. Wei, X. Zhang, J. Wang, S. Zhang, X. Zhang, R. G. Cooks, *Chem. Sci.* **2018**, *9*, 7779–7786.
- [12] C. Liu, J. Li, H. Chen, R. N. Zare, *Chem. Sci.* **2019**, *10*, 9367–9373.
- [13] H. Nie, Z. Wei, L. Qiu, X. Chen, D. T. Holden, R. G. Cooks, *Chem. Sci.* **2020**, *11*, 2356–2361.
- [14] K. Huang, J. Ghosh, S. Xu, R. G. Cooks, *ChemPlusChem* **2022**, *87*, e202100449.
- [15] N. M. Morato, M. T. Le, D. T. Holden, R. G. Cooks, *SLAS Technol.* **2021**, *26*, 555–571.
- [16] C. Salvitti, A. Troiani, F. Mazzei, C. D'Agostino, R. Zumpano, C. Baldacchini, A. R. Bizzarri, A. Tata, F. Pepi, *Int. J. Mass Spectrom.* **2021**, *468*, 116658.
- [17] B. Zheng, X. Jin, J. Liu, H. Cheng, *ACS Sustainable Chem. Eng.* **2021**, *9*, 4383–4390.
- [18] Y. Li, T. F. Mehari, Z. Wei, Y. Liu, R. G. Cooks, *J. Mass Spectrom.* **2020**, *56*, e4585.
- [19] L. Qiu, Z. Wei, H. Nie, R. G. Cooks, *ChemPlusChem* **2021**, *86*, 1362–1365.
- [20] H. Xiong, J. K. Lee, R. N. Zare, W. Min, *J. Phys. Chem. Lett.* **2020**, *11*, 7423–7428.
- [21] K. Leung, *J. Phys. Chem. Lett.* **2010**, *1*, 496–499.
- [22] J. R. Cendagorta, T. Ichiye, *J. Phys. Chem. B* **2015**, *119*, 9114–9122.
- [23] H. Hao, I. Leven, T. Head-Gordon, *Nat. Commun.* **2022**, *13*, 280.
- [24] J. K. Lee, K. L. Walker, H. S. Han, J. Kang, F. B. Prinz, R. M. Waymouth, H. G. Nam, R. N. Zare, *Proc. Natl. Acad. Sci. USA* **2019**, *116*, 19294–19298.
- [25] D. Gao, F. Jin, J. K. Lee, R. N. Zare, *Chem. Sci.* **2019**, *10*, 10974–10978.
- [26] L. Qiu, M. D. Psimos, R. G. Cooks, *J. Am. Soc. Mass Spectrom.* **2022**, *33*, 1362–1367.
- [27] L. Qiu, N. M. Morato, K.-H. Huang, R. G. Cooks, *Front. Chem.* **2022**, *10*, <https://doi.org/10.3389/fchem.2022.903774>.
- [28] J. K. Lee, D. Samanta, H. G. Nam, R. N. Zare, *J. Am. Chem. Soc.* **2019**, *141*, 10585–10589.
- [29] C. Gong, D. Li, X. Li, D. Zhang, D. Xing, L. Zhao, X. Yuan, X. Zhang, *J. Am. Chem. Soc.* **2022**, *144*, 3510–3516.
- [30] D. Ben-Amotz, *Science* **2022**, *376*, 800–801.
- [31] M. Wang, X.-F. Gao, R. Su, P. He, Y.-Y. Cheng, K. Li, D. Mi, X. Zhang, X. Zhang, H. Chen, et al., *CCS Chem.* **2021**, 3559–3566.
- [32] M. A. Pasek, J. M. Sampson, Z. Atlas, *Proc. Natl. Acad. Sci. USA* **2014**, *111*, 15468–15473.
- [33] G. P. Horsman, D. L. Zechel, *Chem. Rev.* **2017**, *117*, 5704–5783.
- [34] S. S. Kamat, H. J. Williams, F. M. Raushel, *Nature* **2011**, *480*, 570–573.
- [35] C. F. Chamberlayne, R. N. Zare, *J. Chem. Phys.* **2020**, *152*, 184702.
- [36] C. F. Chamberlayne, R. N. Zare, *J. Chem. Phys.* **2022**, *156*, 054705.
- [37] K.-H. Huang, Z. Wei, R. G. Cooks, *Chem. Sci.* **2021**, *12*, 2242–2250.
- [38] L. W. Zilch, J. T. Maze, J. W. Smith, G. E. Ewing, M. F. Jarrold, *J. Phys. Chem. A* **2008**, *112*, 13352–13363.
- [39] A. Tholey, J. Reed, W. D. Lehmann, *J. Mass Spectrom.* **1999**, *34*, 117–123.
- [40] R. F. Hudson, L. Keay, *J. Chem. Soc.* **1956**, 2463.
- [41] Q. Wan, S. Chen, A. K. Badu-Tawiah, *Chem. Sci.* **2018**, *9*, 5724–5729.
- [42] A. T. Blades, M. G. Ikonou, P. Kebarle, *Anal. Chem.* **1991**, *63*, 2109–2114.
- [43] S. Tang, H. Cheng, X. Yan, *Angew. Chem. Int. Ed.* **2020**, *59*, 209–214; *Angew. Chem.* **2020**, *132*, 215–220.
- [44] R. M. Bain, C. J. Pulliam, R. G. Cooks, *Chem. Sci.* **2015**, *6*, 397–401.
- [45] L. Feng, X. Yin, S. Tan, C. Li, X. Gong, X. Fang, Y. Pan, *Anal. Chem.* **2021**, *93*, 15775–15784.
- [46] Y. Gauduel, S. Pommeret, A. Migus, A. Antonetti, *Chem. Phys.* **1990**, *149*, 1–10.
- [47] J. Ma, F. Wang, M. Mostafavi, *Molecules* **2018**, *23*, 244.
- [48] J. Ma, U. Schmidhammer, P. Pernot, M. Mostafavi, *J. Phys. Chem. Lett.* **2014**, *5*, 258–261.

Manuscript received: July 21, 2022

Accepted manuscript online: August 22, 2022

Version of record online: September 7, 2022